J. Plasma Physics (1999), *vol.* 62, *part* 1, *pp.* 87–94. Printed in the United Kingdom

© 1999 Cambridge University Press

Electromagnetic wave propagation in a chiroplasma-filled waveguide

J. GONG

Bei Yuan 1302, Southwest Jiaotong University, Chengdu, 610031, P.R.China

(Received 16 September 1998 and in revised form 30 November 1998)

Abstract. A dispersion equation is derived for a cylindrical waveguide of circular cross-section partially filled with chiroplasma. The propagation characteristics of electromagnetic waves in the family of waveguide modes are studied. The dispersion curves are given. It is found that the propagation constant changes almost linearly with the chirality admittance for the parameters that we choose, and increases with increasing filled area.

1. Introduction

Chiral media, characterized by an intrinsic left- or right-handedness at optical frequencies due to a natural helical structure, have been known in optics under the more common name of optically active materials. There has been renewed interest in such media because of the possibility that their characteristics might be extended to microwave or millimetre wavelengths through advances in polymer science or through the manufacture of artificial dielectrics (Jaggard 1979).

Extensive investigations of electromagnetic chirality in a large number of applications included a study of the effect of electromagnetic chirality in guided-wave structures (Engheta and Pelet 1989). In order to achieve control of chirality in guided-wave structures, certain forms of anisotropy must be introduced. A chiroplasma, consisting of chiral objects embedded in a magnetically biased plasma, is one of the possible candidates. Here we study the propagation characteristics of electromagnetic waves in a cylindrical waveguide partially filled with a chiroplasma, since this kind of waveguide is often used in microwave electronics.

2. Dispersion equation and propagation characteristics

For the chiroplasma, we select

$$\mathbf{D} = \boldsymbol{\varepsilon}\cdot\mathbf{E} + i\xi_c\mathbf{B}, \qquad \mathbf{H} = i\xi_c\mathbf{E} + \frac{\mathbf{B}}{\mu}$$

as the appropriate form of the constitutive relations (Engheta et al. 1992), where

$$\boldsymbol{\varepsilon} = \begin{bmatrix} \varepsilon & -ig & 0 \\ ig & \varepsilon & 0 \\ 0 & 0 & \varepsilon_z \end{bmatrix}$$

https://doi.org/10.1017/S0022377899007692 Published online by Cambridge University Press

is the dielectric tensor, μ is the scalar permeability and ξ_c is the chirality admittance.

$$\frac{\varepsilon}{\varepsilon_1} = 1 - \frac{\omega_p^2}{\omega^2 - \omega_c^2},$$

$$\frac{g}{\varepsilon_1} = \frac{\omega_p^2 \omega_c}{\omega(\omega^2 - \omega_c^2)}$$

and

$$\frac{\varepsilon_z}{\varepsilon_1} = 1 - \frac{\omega_p^2}{\omega^2}$$

are modified forms of the expressions for a collisionless biased plasma, where ε_1 is the high-frequency permittivity of the medium when ξ_c goes to zero. ω is the wave frequency, $\omega_p = (4\pi e^2 n_c/m)^{1/2}$ is the plasma frequency and $\omega_c = eB_0/cm$ is the electron cyclotron frequency.

We assume that all the electromagnetic waves have a factor $\exp[i(\omega t - \beta z)]$, where β is the propagation constant.

Manipulating the source-free Maxwell equations, we get the following coupled wave equations:

$$\nabla_t^2 E_z + p_1 E_z + i p_2 H_z = 0, \tag{1}$$

$$\nabla_t^2 H_z + i p_3 E_z + p_4 H_z = 0. \tag{2}$$

These two equations are coupled to each other because H_z enters (1) and E_z enters (2); therefore the wave equation for E_z or H_z is of fourth order. The wave coefficients in (1) and (2) are

$$p_1 = \frac{\varepsilon_z}{\varepsilon}(\omega^2\mu\varepsilon - \beta^2) + \omega\mu\xi_c\left(\frac{\beta g}{\varepsilon} + 2\omega\mu\xi_c\right),$$

$$p_2 = \omega\mu\left(\frac{\beta g}{\varepsilon} + 2\omega\mu\xi_c\right),$$

$$p_3 = \beta^2\xi_c\left(1 - \frac{\varepsilon_z}{\varepsilon}\right) - \omega\left[\omega\mu\xi_c\left(\varepsilon + \varepsilon_z + 2\mu\xi_c^2 - \frac{g^2}{\varepsilon}\right) + \frac{g\beta}{\varepsilon}(\varepsilon_z - \mu\xi_c^2)\right],$$

$$p_4 = \omega^2\mu\varepsilon - \beta^2 + \omega\mu\left(2\omega\mu\xi_c^2 - g\frac{\omega g + \beta\xi_c}{\varepsilon}\right).$$

We use subscripts t and z to denote the transverse and longitudinal components of the waves.

The relations between the transverse and longitudinal components of the waves are obtained from the Maxwell equations as follows:

$$\mathbf{E}_t = ia\boldsymbol{\nabla}_t E_z + b\boldsymbol{\nabla}_t E_z \times \mathbf{a}_z + c\boldsymbol{\nabla}_t H_z + id\boldsymbol{\nabla}_t H_z \times \mathbf{a}_z, \tag{3}$$

$$\mathbf{H}_t = e\boldsymbol{\nabla}_t E_z + if\boldsymbol{\nabla}_t E_z \times \mathbf{a}_z + ia\boldsymbol{\nabla}_t H_z + b\boldsymbol{\nabla}_t H_z \times \mathbf{a}_z, \tag{4}$$

where a, b, c, d, e and f are given by

$$a = \frac{p_3\omega\mu g - p_4(\beta\varepsilon_z - \omega\mu\xi_c g)}{\varepsilon(p_1 p_4 + p_2 p_3)},$$

$$b = -\frac{\omega\mu(p_3 + \xi_c p_4)}{p_1 p_4 + p_2 p_3},$$

https://doi.org/10.1017/S0022377899007692 Published online by Cambridge University Press

$$c = -\frac{p_1 \omega\mu g + p_2(\beta\varepsilon_z - \omega\mu\xi_c g)}{\varepsilon(p_1 p_4 + p_2 p_3)},$$

$$d = -\frac{\omega\mu(p_1 - \xi_c p_2)}{p_1 p_4 + p_2 p_3},$$

$$e = -\frac{p_3(\beta\varepsilon + \omega\mu\xi_c g) + p_4 \xi_c[\beta(\varepsilon - \varepsilon_z) + \omega\mu\xi_c g]}{\varepsilon(p_1 p_4 + p_2 p_3)},$$

$$f = \frac{\omega[p_3 \mu\xi_c + p_4(\varepsilon_z + \mu\xi_c^2)]}{p_1 p_4 + p_2 p_3}.$$

It is evident that (1) and (2) reduce to the equations for plasma waveguides when $\xi_c = 0$, they reduce to the equations for chirowaveguides when $\omega_p = 0$, and they reduce to decoupled Helmholtz equations for conventional waveguides filled with achiral media when both ξ_c and ω_p are zero.

Equations (3) and (4) take their particular forms because the transverse components are related to the longitudinal components in terms of the coefficients of the wave equations p_1, p_2, p_3 and p_4. For example, when ξ_c and ω_p are zero, one can get

$$\mathbf{E}_t = -\frac{i(\beta\boldsymbol{\nabla}_t E_z + \omega\mu\boldsymbol{\nabla}_t H_z \times \mathbf{a}_z)}{\omega^2\mu\varepsilon - \beta^2},$$

$$\mathbf{H}_t = \frac{i(\omega\varepsilon\boldsymbol{\nabla}_t E_z \times \mathbf{a}_z - \beta\boldsymbol{\nabla}_t H_z)}{\omega^2\mu\varepsilon - \beta^2}$$

from (3) and (4), which are just the relations for a conventional dielectric-filled waveguide.

The above equations are valid for cylindrical waveguides of arbitrary cross-section because we have not used any coordinate system in our derivation.

We consider a cylindrical waveguide of circular cross-section partially filled with a chiroplasma. The axis of the waveguide coincides with the axis of a cylindrical coordinate system $(r, \ , z)$. The waveguide is divided into two layers: region 1, $0 \leqslant r \leqslant R_1$, is filled with the chiroplasma, and region 2, $R_1 \leqslant r \leqslant R_2$, is filled with vacuum.

Solving the coupled equations (1) and (2) in region 1, we have

$$E_{z1} = [AJ_n(s_+ r) + BJ_n(s_- r)]\, e^{in} \qquad (0 \leqslant r \leqslant R_1), \tag{5}$$

$$H_{z1} = i[Ag_+ J_n(s_+ r) + Bg_- J_n(s_- r)]\, e^{in} \qquad (0 \leqslant r \leqslant R_1), \tag{6}$$

where $J_n(x)$ is the nth-order Bessel function of the first kind,

$$s_\pm^2 = \tfrac{1}{2}\{p_1 + p_4 \pm [(p_1 - p_4)^2 - 4p_2 p_3]^{1/2}\},$$

$$g_\pm = \frac{p_1 - s_\pm^2}{p_2}.$$

In region 2, solving the conventional Helmholtz equations for E_z and H_z, we have

$$E_{z2} = C[J_n(k_c r)\, Y_n(k_c R_2) - J_n(k_c R_2)\, Y_n(k_c r)]\, e^{in} \qquad (R_1 \leqslant r \leqslant R_2), \tag{7}$$

$$H_{z2} = D[J_n(k_c r)\, Y_n'(k_c R_2) - J_n'(k_c R_2)\, Y_n(k_c r)]\, e^{in} \qquad (R_1 \leqslant r \leqslant R_2), \tag{8}$$

https://doi.org/10.1017/S0022377899007692 Published online by Cambridge University Press

where $Y_n(x)$ is the nth-order Bessel function of the second kind and $k_c^2 = \omega^2\mu_2\varepsilon_2 - \beta^2$, with μ_2 the vacuum permeability. Subscripts 1 and 2 denote regions 1 and 2 respectively. Because the solutions (5)–(8) have four unknown constants A, B, C and D, we need four linearly independent equations. Using boundary conditions at the chiroplasma surface,

$$E_{z1} = E_{z2}, \quad E_{\theta 1} = E_{\theta 2}, \quad H_{z1} = H_{z2}, \quad H_{\theta 1} = H_{\theta 2} \quad \text{at } r = R_1,$$

we obtain four homogeneous algebraic equations for these constants. For non-trivial solutions, their coefficient determinant must be zero:

$$\begin{vmatrix} a_{1+} & a_{1-} & a_{13} & a_{14} \\ a_{2+} & a_{2-} & a_{23} & a_{24} \\ a_{3+} & a_{3-} & 0 & a_{34} \\ a_{4+} & a_{4-} & a_{43} & 0 \end{vmatrix} = 0, \tag{9}$$

where

$$a_{1\pm} = -\frac{nJ_n(s_\pm R_1)\,(a + cg_\pm)}{R_1} + s_\pm J_n'(s_\pm R_1)\,(-b + dg_\pm),$$

$$a_{13} = -\frac{n\beta[J_n(k_cR_1)\,Y_n(k_cR_2) - J_n(k_cR_2)\,Y_n(k_cR_1)]}{k_c^2 R_1},$$

$$a_{14} = \frac{\omega\mu_2[J_n'(k_cR_1)\,Y_n'(k_cR_2) - J_n'(k_cR_2)\,Y_n'(k_cR_1)]}{k_c},$$

$$a_{2\pm} = \frac{nJ_n(s_\pm R_1)\,(e - ag_\pm)}{R_1} - s_\pm J_n'(s_\pm R_1)\,(f + bg_\pm),$$

$$a_{23} = \frac{\omega\varepsilon_2[J_n'(k_cR_1)\,Y_n(k_cR_2) - J_n(k_cR_2)\,Y_n'(k_cR_1)]}{k_c},$$

$$a_{24} = -\frac{n\beta[J_n(k_cR_1)\,Y_n'(k_cR_2) - J_n'(k_cR_2)\,Y_n(k_cR_1)]}{k_c^2 R_1},$$

$$a_{3\pm} = g_\pm J_n(s_\pm R_1),$$

$$a_{34} = -J_n(k_cR_1)\,Y_n'(k_cR_2) + J_n'(k_cR_2)\,Y_n(k_cR_1),$$

$$a_{4\pm} = J_n(s_\pm R_1),$$

$$a_{43} = -J_n(k_cR_1)\,Y_n(k_cR_2) + J_n(k_cR_2)\,Y_n(k_cR_1).$$

3. Analysis of the dispersion relation

Equation (9) is a dispersion relation for the waveguide. It turns out to be a dispersion relation of a waveguide fully filled with a chiroplasma when $R_1 = R_2$.

Before considering this equation, we discuss the following. It is well known that mode classification in normal vacuum waveguides is in terms of the cut-off wavenumber k_c. s_+^2 is like k_c in this respect. For a plasma waveguide, the (ω, β) plane can be divided into three possible regions: $s_\pm^2 > 0$, $s_\pm^2 < 0$ or $s_\pm^2$ complex. The solutions (5) and (6) in these regions differ substantially, i.e. the solutions depend on $s_\pm^2$. The region boundaries do not depend on the chiroplasma radius or the waveguide radius.

https://doi.org/10.1017/S0022377899007692 Published online by Cambridge University Press

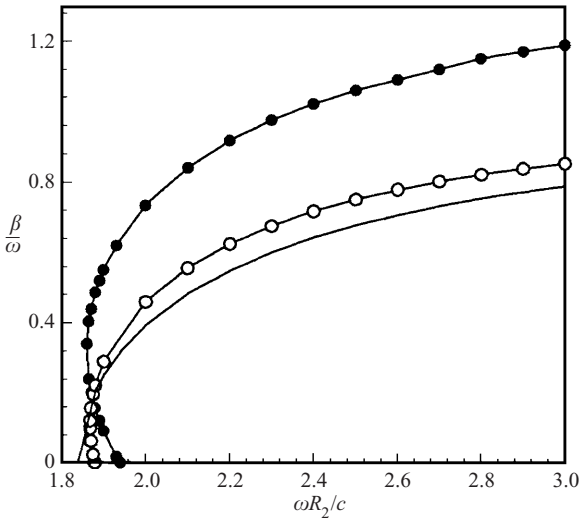


Figure 1. Normalized dispersion diagram of the HE_{11} mode for $\omega_c R_2/c = 1$, $\omega p R_2/c = 1$, $\xi_e = 0.001\,\mathrm{S}$, $R_1/R_2 = 0.5$ and $\varepsilon_1 = \varepsilon_2 = \varepsilon_0$: ——, vacuum waveguide; ○—○, partially filled waveguide; ●—●, fully filled waveguide.

From previous work on plasma waveguides (Bevc and Everhart 1962; Ivanov and Alexov 1990), we know that there are three families of waves in the regions where at least one of s_+^2 or s_-^2 is positive: plasma EH^p modes with $\omega < \min(\omega_p,\ \omega_c)$, cyclotron HE^c modes with $\min(\omega_p,\ \omega_c) < \omega < \omega_h$ $(\omega_h = (\omega_p^2 + \omega_c^2)^{1/2})$ and waveguide EH $(\omega > \omega_p)$ and HE $(\omega > \omega_h)$ modes. It should be noted that the lower-frequency limits of the HE^c-cyclotron modes and the waveguide HE and EH modes are given only approximately.

These classifications are not appropriate for the present case. However, they do give very rough views of it. Here we restrict our attention to the waveguide modes.

We know that all modes are hybrid from (1) and (2). Therefore the description EH_{nm} is used for modes originating in achiral TM_{nm} modes, and HE_{nm} for modes stemming from achiral TE_{nm} modes. Here n and m denote the azimuthal and radial mode numbers, where n implies an azimuthal variation and m implies that the mode is number m when ordered after increasing cutoff frequency for given n.

The propagation curves of the HE_{11} and EH_{01} modes are plotted in Figs 1 and 2 respectively. In order to reveal the propagation characteristics more clearly, we also calculate the propagation curves of the vacuum and fully filled chiroplasma waveguides as comparisons. As can be seen from Figs 1 and 2, the cut-off frequency of the HE_{11} mode shifts towards a frequency higher than that of the vacuum TE_{11}, and the cut-off frequency of the EH_{01} mode shifts towards a lower frequency. This shows that the influences of the chiroplasma on modes are different. A characteristic common to both the HE_{11} and EH_{01} modes is that the partially filled curves lie between the fully filled and the vacuum curves. This phenomenon can be explained by coupled-wave theory. The partially filled chiroplasma causes a partial coupling between the fully filled chiroplasma and vacuum waveguides, resulting in the β of the partially filled waveguide being higher than that of the vacuum one, but lower than that of the fully filled one.

https://doi.org/10.1017/S0022377899007692 Published online by Cambridge University Press

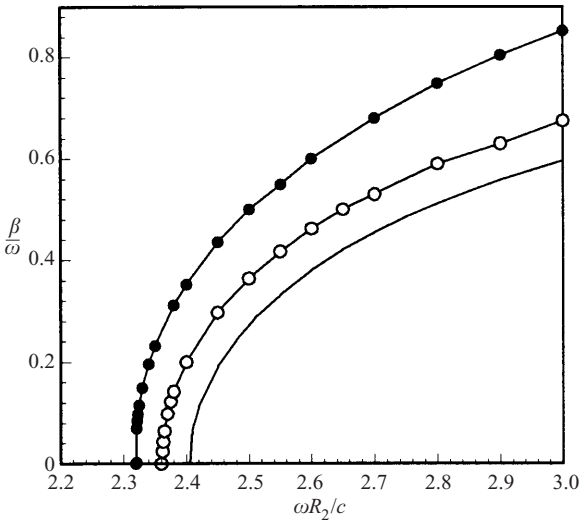


Figure 2. Normalized dispersion diagram of the EH_{01} mode for $\omega_c R_2/c = 1$, $\omega_p R_2/c = 1$, $\xi_c = 0.001\,\mathrm{S}$, $R_1/R_2 = 0.5$ and $\varepsilon_1 = \varepsilon_2 = \varepsilon_0$: ——, vacuum waveguide; ○—○, partially filled waveguide; ●—●, fully filled waveguide.

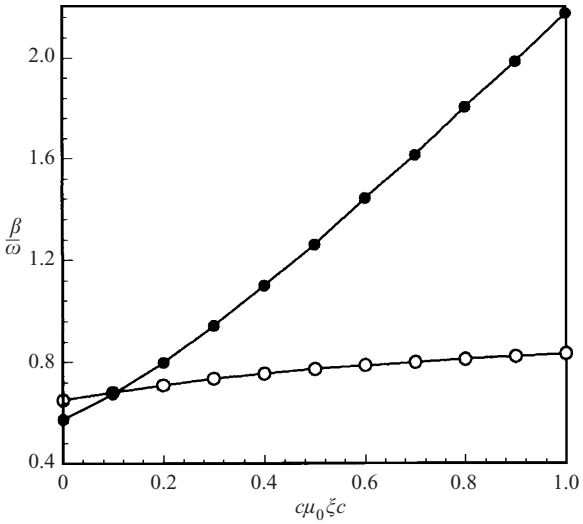


Figure 3. Variation of the propagation constant of the HE_{11} mode with the chirality admittance for $\omega R_2/c = 2.5$, $\omega_c R_2/c = 1$, $\omega_p R_2/c = 1$, $R_1/R_2 = 0.5$ and $\varepsilon_1 = \varepsilon_2 = \varepsilon_0$: ○—○, partially filled waveguide; ●—●, fully filled waveguide.

We can also see that the partially filled curves are closer to the vacuum ones, because the filled region is smaller than the vacuum region with $R_1 = 0.5$. When the filled region is small, the coupling between the medium and the waveguide is small, and therefore the dispersion curve of the partially filled waveguide is close to the vacuum-waveguide one. When the filled region increases, the coupling will increase, and therefore the dispersion curve will shift up away from the vacuum one.

Figures 3 and 4 show how β changes with the chirality admittance. We can

https://doi.org/10.1017/S0022377899007692 Published online by Cambridge University Press

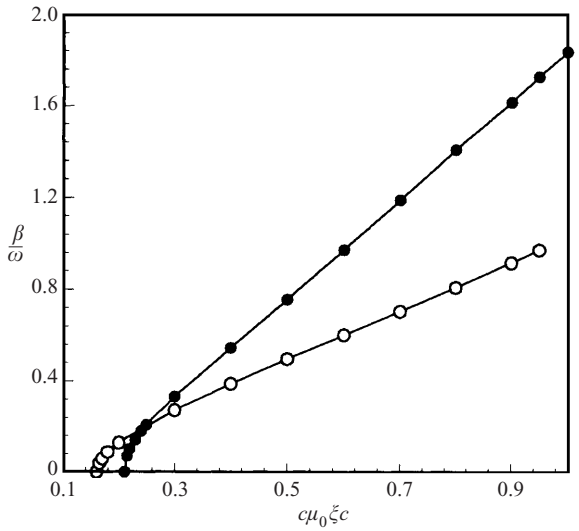


Figure 4. Variation of the propagation constant of the EH_{01} mode with the chirality admittance for $\omega R_2/c = 2.5$, $\omega_c R_2/c = 1$, $\omega_p R_2/c = 1$, $R_1/R_2 = 0.5$ and $\varepsilon_1 = \varepsilon_2 = \varepsilon_0$: ○—○, partially filled waveguide; ●—●, fully filled waveguide.

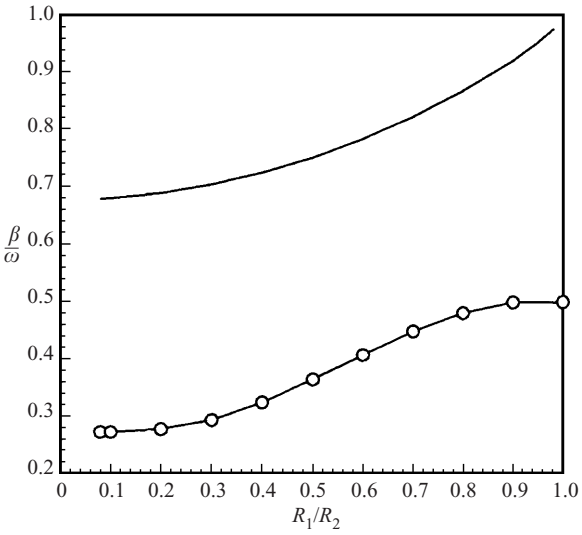


Figure 5. Variation of the propagation constants of the HE_{11} (——) and EH_{01} (○—○) modes with the filled area for $\omega R_2/c = 2.5$, $\omega_c R_2/c = 1$, $\omega_p R_2/c = 1$, $\xi_c = 0.001$ S and $\varepsilon_1 = \varepsilon_2 = \varepsilon_0$.

see that β increases almost linearly with ξ_c for both the HE_{11} and EH_{01} modes. The partially filled curves in both cases are below the fully filled ones. The reason is the same as discussed above.

Figure 5 shows how β changes with the filled area. We can see that β increases with R_1. This is because the coupling between the chiroplasma and the vacuum waveguides increases with increasing filled area, and β increases with the coupling. When R_1 approaches R_2, β tends to the value of β for the fully filled curves at $\omega R_2/c = 2.5$, as can be seen in Figs 1 and 2.

https://doi.org/10.1017/S0022377899007692 Published online by Cambridge University Press

4. Conclusions

The wave equations for E_z and H_z have been derived for waveguides of arbitrary cross-section filled with a chiroplasma. The relations between the transverse and longitudinal components of the electromagnetic field have also been given. These take their particular forms because the relations between the transverse and longitudinal components are expressed in terms of the coefficients of the wave equations.

The dispersion relation has been derived for a cylindrical waveguide of circular cross-section partially filled with a chiroplasma in order to study the propagation characteristics of the electromagnetic wave. We have solved the equation in the context of the family of the waveguide modes. From the solutions of the equation, the propagation characteristics of the waves can be clearly revealed. It is found that the propagation constant changes almost linearly with the chirality admittance for the chosen parameters. This characteristic might give this waveguide great potential for application in the further development of microwave electronics. For example, it could be expected to be applied in a cyclotron autoresonance maser. Using the chirality admittance to adjust the resonant point of the forward wave, it should be possible to avoid backward wave oscillation in the maser.

Acknowledgement

This work was supported financially by the National Natural Science Foundation of China under Contract 69508004.

References

Bevc, V. and Everhart, T. E. 1962 *J. Electron. Control* **13**, 185.

Engheta, N. and Pelet, P. 1989 *Opt. Lett.* **14**, 593.

Engheta, N., Jaggard, D. L. and Kowarz, M. W. 1992 *IEEE Trans. Antennas Propagation* **40**, 367.

Ivanov, S. T. and Alexov, E. G. 1990 *J. Plasma Phys.* **43**, 51.

Jaggard, D. L., Mickelon, A. R. and Papas, C. H. 1979 *Appl. Phys.* **18**, 211.

https://doi.org/10.1017/S0022377899007692 Published online by Cambridge University Press